



## Resistive states created in superconducting NbTiN filaments by an electrical current pulse

K. Harrabi

Citation: *AIP Advances* **5**, 037102 (2015); doi: 10.1063/1.4914103

View online: <http://dx.doi.org/10.1063/1.4914103>

View Table of Contents: <http://scitation.aip.org/content/aip/journal/adva/5/3?ver=pdfcov>

Published by the *AIP Publishing*

---

### Articles you may be interested in

[Terahertz electrodynamics and superconducting energy gap of NbTiN](#)

*J. Appl. Phys.* **114**, 243905 (2013); 10.1063/1.4856995

[NbTiN superconducting nanowire detectors for visible and telecom wavelengths single photon counting on Si<sub>3</sub>N<sub>4</sub> photonic circuits](#)

*Appl. Phys. Lett.* **102**, 051101 (2013); 10.1063/1.4788931

[Enhanced telecom wavelength single-photon detection with NbTiN superconducting nanowires on oxidized silicon](#)

*Appl. Phys. Lett.* **96**, 221109 (2010); 10.1063/1.3428960

[Time-Resolved Far-Infrared Studies of Superconducting Nb<sub>0.5</sub>Ti<sub>0.5</sub>N Film in a Magnetic Field](#)

*AIP Conf. Proc.* **850**, 981 (2006); 10.1063/1.2355034

[Low-noise submillimeter-wave NbTiN superconducting tunnel junction mixers](#)

*Appl. Phys. Lett.* **75**, 4013 (1999); 10.1063/1.125522

---

The advertisement features a row of computer monitors in a library setting, each displaying the cover of the journal 'Computing - Science & Engineering'. The covers show a colorful, abstract pattern. The text 'Computing - Science & Engineering' is visible on the covers. Below the monitors, the text 'AIP'S JOURNAL OF COMPUTATIONAL TOOLS AND METHODS. AVAILABLE AT MOST LIBRARIES.' is displayed in a large, white, sans-serif font. The 'Computing - Science & Engineering' logo is also present in the bottom right corner of the advertisement.

## Resistive states created in superconducting NbTiN filaments by an electrical current pulse

K. Harrabi

Physics Department, King Fahd University of Petroleum and Minerals,  
31261 Dhahran, Saudi Arabia

(Received 31 January 2015; accepted 21 February 2015; published online 2 March 2015)

We have observed as a function of the time the appearance of the voltage caused by a larger-than-critical ( $I > I_c$ ) step-pulse of current in narrow NbTiN strips at 4.2 K. Different current intensities produced either phase-slip centres characterized by a voltage saturating with the time, or ever expanding hot spots. These dissipative structures occur after a measurable delay time, whose dependence upon the ratio  $I/I_c$  can be analysed through a Ginzburg-Landau theory to yield a unique adjustable time constant. © 2015 Author(s). All article content, except where otherwise noted, is licensed under a Creative Commons Attribution 3.0 Unported License. [<http://dx.doi.org/10.1063/1.4914103>]

### I. INTRODUCTION

In a superconducting nanowire single photon detector (SSND), the photon absorption leads to the destruction of the superconductivity, eventually recorded as a voltage signal in a current-biased device. More exactly, the excitation coming from the initial absorption spot spreads across the width of the sample, thereby squeezing the current lines until the critical current density  $J_c$  is reached, and a normal zone (or hot spot) is formed.<sup>1</sup> In this way, the process of detection bears some similarity with the spontaneous creation of resistive centres by an over-critical current pulse. Both phenomena are even combined in the parallel nanowire detector,<sup>2</sup> where the first capture by one of the wires is followed by an increase of the current in the other ones, and the subsequent creation of resistive centres. However, the resistive spots created spontaneously occur retarded by a delay time  $t_d$  compared to the current pulse. The measurement of that quantity and its interpretation will be the main subject of this paper.

Some features of non-equilibrium superconductivity have been describes a long time ago.<sup>3,4</sup> When driven by a current  $I$  larger than the pair-breaking critical  $I_c$ , a superconducting filament develops resistance in a localized spots, namely localized phase-slip centres (PSC) and hot spots (HS). According to the standard model,<sup>3,4</sup> a PSC is a localized quantum dissipation unit where a zone periodically alternates in time between normal and superconducting states. Our purpose in this work is to study the creation of these resistive states in the time domain for the first time in superconducting nitride  $Nb_xTi_{1-x}N$ . Studies in different materials such as Nb and YBCO were reported before.<sup>5,6</sup> Then, a Time Dependent Ginzburg Landau theory (TDGL) allows to derive the heat escape time, an essential information about the performance and the efficiency of SSND, since it is related to its recovery time. In addition, a model calculation is proposed to describe the appearance of the dissipative states as a function of the time.

### II. EXPERIMENTAL SET-UP

Our NbTiN film, 150 nm thick, was deposited at room temperature on sapphire by DC magnetron sputtering in an argon-nitrogen plasma (STAR-Cryoelectronics, NM, USA). The final pattern, including two lateral probes, 1 mm apart from one another, plus four contact pads, was obtained by using standard photo-lithographic processes and ion milling. The measurements were performed at 4.2 K on three samples CEw3, CEw5 and CEw10, corresponding to three different widths  $w = 3, 5$



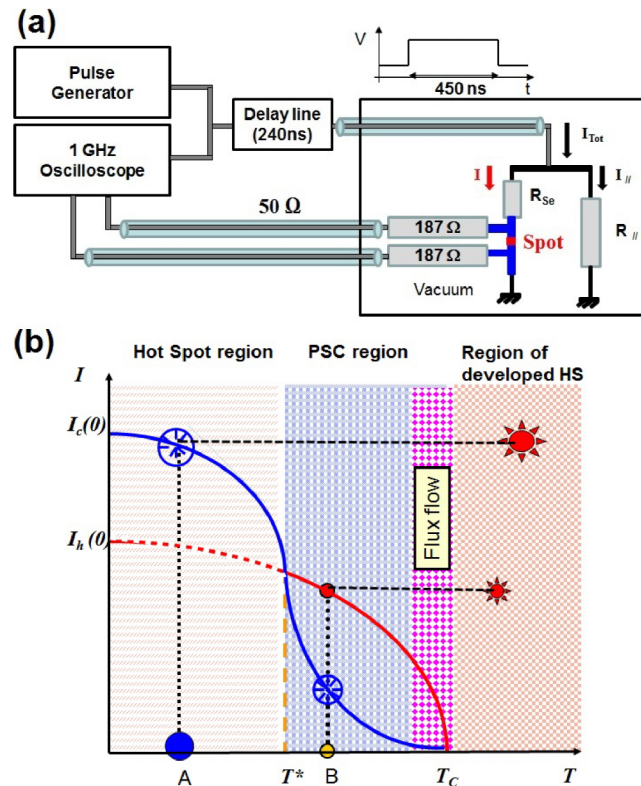


FIG. 1. (a) Measurement set-up showing the 50  $\Omega$ -delay line used to separate in time the incident from the reflected pulse. The pulse generator is equipped with an external attenuator (not shown) varying by 0.1 dB steps. In insert, the resistances in parallel ( $R_{||} = 67 \Omega$ ) and series ( $R_{se} = 187 \Omega$ ) are chosen to provide a 50  $\Omega$  termination to the incident excitation. (b) Sketch of the current-temperature state diagram showing different dissipative regimes of HS, PSC and flux flow.

and 10  $\mu\text{m}$ . The critical temperatures  $T_c$  were respectively 8.3 K, 8.7 K, and 9 K. The resistivities at 20 K were found to be  $\rho(20 \text{ K}) = 182, 176, \text{ and } 163 \mu\Omega\cdot\text{cm}$ .

The superconducting strip receives from a pulse generator electrical pulses of 450 ns duration and 10 kHz repetition rate. 50  $\Omega$  coaxial cables and a delay line were used for the pulse measurement (Fig. 1). A quasi-constant current pulse flowing into the sample is insured by using the combination of  $R_{||}$  and  $R_{se}$  ( $R_{||} = 67 \Omega$  and  $R_{se} = 187 \Omega$ ), equivalent to a 50  $\Omega$  impedance at the line's termination. The current passing through the sample is  $I = I_{Tot} \cdot R_{||} / (R_{||} + R_{se})$ , with  $I_{Tot} = \frac{V_i}{Z}$  ( $V_i$  is the input voltage,  $Z = 50 \Omega$ ). The voltage response was recorded using a fast oscilloscope through lateral electrodes with 187  $\Omega$  connected in series (Fig. 1).

### III. CHARACTERIZATION OF THE SPOT INDUCED BY A CURRENT PULSE

The PSC occurs in a wide superconducting filament ( $w \gg \xi$ ) considered as two dimension, where the order parameter behaves similarly compared to one dimension ( $w \approx \xi$ ).<sup>9</sup> We have studied the time evolution of this behaviour by using current step-pulses. Different dissipative modes appeared based on the applied current pulse amplitude.<sup>14</sup> The destruction of the superconductivity occurs at a region where the filament presented a weak link or defect. However, the nature of dissipation depends on different parameters, and can be transcribed to the temperature dependence of two currents  $I_c(T)$  and  $I_h(T)$ .<sup>5-8</sup> Here  $I_c$  is the critical current which initiates the dissipation (it is defined experientially as the current which leads to the longest achievable  $t_d$ ). On the other hand,  $I_h$  is the minimum current amplitude able to maintain a steady HS above the critical temperature  $T_c$ . The voltage response to an electrical pulse presents a delay time  $t_d$ , depending on the film properties. According to the value of the working temperature  $T$  compared to  $T^*$ , the temperature

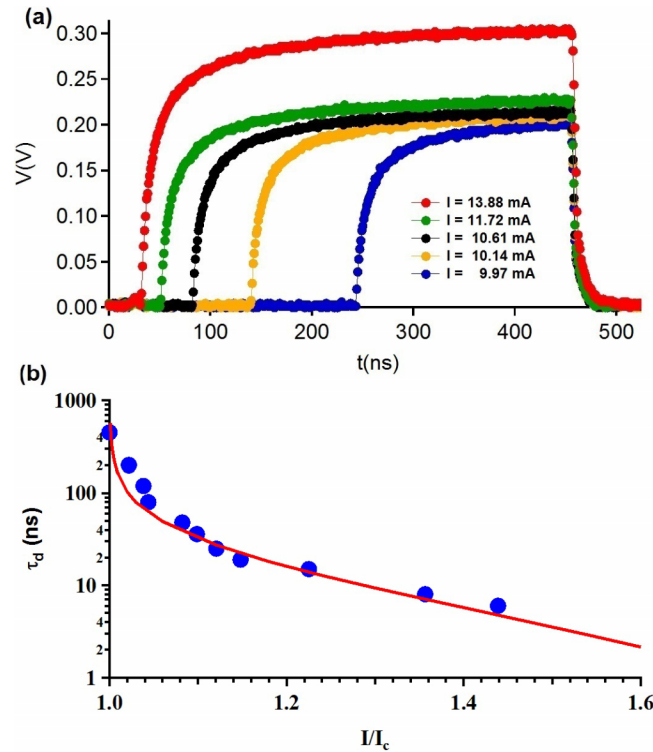


FIG. 2. (a) Voltage response vs time of sample CEw3 for  $I > I_c$  at  $T = 4.2$  K. (b) Delay time vs  $I/I_c$  and fitting (continuous trace) with Tinkham's TDGL theory.<sup>4</sup>

that makes  $I_c(T^*) = I_h(T^*)$ . Two behaviours are expected.<sup>6</sup>  $T > T^*$  (see point B in Fig. 1(b)) leads to the nucleation of a PSC. However,  $T < T^*$  (see point A in Fig. 1(b)) leads to the formation of a HS.

A typical set of responses to an electrical pulse excitation is shown in Fig. 2(a) of film CEw3. The raise of voltage which marks the destruction of superconductivity occurs after a delay time  $t_d$  for a current pulse amplitude exceeding the critical value ( $I_c = 9$  mA for  $T = 4.2$  K). The measurement showing an un-saturating voltage over more than 400 ns, it cannot correspond to a PSC. We conclude that it corresponds a HS voltage, and therefore  $T^*$  is larger than  $T$ . The existence of the delay time and its dependence upon the ratio  $I/I_c$  has been discovered and interpreted by Pals and Wolter,<sup>10</sup> on the basis of a TDGL equation. This study led to the relation:

$$t_d(I/I_c) = \tau_d \int_0^1 \frac{2f^4 df}{\frac{4}{27}(\frac{I}{I_c})^2 - f^4 + f^6} \quad (1)$$

The fitting parameter  $\tau_d$ , was first interpreted as the gap relaxation time, related to electron-phonon inelastic time. Later a generalized theory<sup>3</sup> included a temperature dependence, which causes  $t_d$  to depend on the two variables  $(T/T_c)$  and  $(I/I_c)$ . Even though this theory has been designed for the time of nucleation of PSCs, it has been shown<sup>6</sup> that it remains valid for the time of formation of HSs. In Fig. 2(b), where the experimental data are plotted as dots we fit the Tinkham function corresponding to  $T/T_c \approx 0.3$  by adjustment of the pre-factor  $\tau_d$  (in the present case for CEw3,  $\tau_d = 5$  ns).

The variety of resistive states resulting from the application of  $I > I_c$  is illustrated in Fig. 3, by the contrast between traces 3a (sample CEw5) and traces 3-b (sample CEw10). While the voltages of the 3b keep increasing long after  $t_d$ , revealing the expansion of a normal HS, the traces 3a show definitely a saturated voltage, typical of a stable PSC. Consistently with this conclusion a plot of the plateau voltages (Fig. 3(a) right) as a function of the amplitudes  $I$  shows a linear dependence extrapolating to  $V = 0$  at a value of the current  $I_s = 12$  mA, known as the excess superconducting current.<sup>3</sup> On the other hand, the voltages of CEw10 do not show the same trend. The difference of

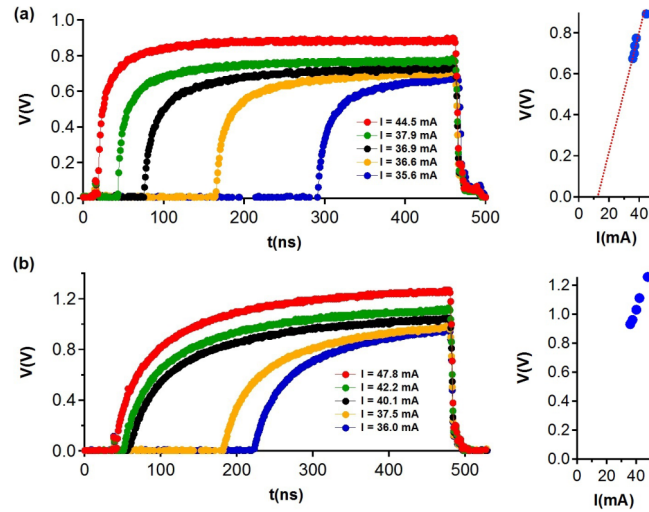


FIG. 3. (a) Voltage response of CEw5 sample to current pulses as a function of time at  $T = 4.2$  K. The stable voltage *vs* time shows the nucleation of a PSC. The right plot illustrates the PSC voltage *vs* the applied current amplitude, where the excess current  $I_s = 12$  mA. (b) Time dependence of voltage across CEw10 in response to a rectangular current pulse at  $T = 4.2$  K. The dependence of the voltage *vs* time shows the growth of the HS. Right graph: plot of the HS voltage *vs* the applied current amplitude.

behaviours (PSC *versus* HS) between CEw5 and CEw10 is to be attributed to different  $T^*$ s ( $T^* < 4.2$  K for CEw5 and  $T^* > 4.2$  K for CEw10).

For sample CEw10, the extrapolation of the voltages (taken at  $t = 450$  ns) seemingly points to the origin ( $V = 0$ ;  $I = 0$ ). However, we think that is a misleading coincidence resulting from the compensation of two tendencies: an upward curvature due to the geometrical expansion of the hotspot, and a decrease of the current (downward curvature) due to the inability of the circuitry to insure perfect control of the current through the changes of the load.

Finally, these dynamic measurements reveal a supplementary information. The fitting of the delay times with Tinkham analysis<sup>3</sup> defines the pre-factor  $\tau_d$  of Eq. (1). In some experiments, it has been identified with the cooling time of the superconducting film, apt to explain the temperatures of HSs and PSCs in current driven Nb<sup>6</sup> and YBCO.<sup>15</sup> If we apply the same principle to present case, we find cooling times  $\tau_d = 5, 6$  and  $5.5$  ns for samples CEw3, CEw5 and CEw10 respectively, which average to  $5.5$  ns for a common thickness  $150$  nm. These times are over estimated due to the limited rise-time of the pulse generator. Nevertheless, we can deduce equivalently, the upper limit of cooling time of sputtered NbTiN on sapphire can be expressed by  $\tau_d \leq 37$  ps/nm thickness.

#### IV. REPRODUCIBILITY OF EXPERIMENT RESULTS NUMERICALLY

A recent theoretical work<sup>11</sup> based on the Kramer and Watts-Tobin equations<sup>12</sup> allows to study in two dimensions the evolution of a superconducting filament driven by a current varying in time. We have attempted to adapt this calculation to our experimental situation of a superconducting filament excited by a current pulse and in the absence of an external magnetic field. The simulations were performed by solving numerically the time-dependent Ginzburg-Landau equations:<sup>12</sup>

$$\frac{u}{\sqrt{1 + \gamma^2 |\psi|^2}} \left( \frac{\partial}{\partial t} + \frac{\gamma^2}{2} \frac{\partial |\psi|^2}{\partial t} \right) = (\nabla - i\mathbf{A})^2 \psi + (1 - |\psi|^2) \psi, \quad (2)$$

$$\frac{\partial \mathbf{A}}{\partial t} = \text{Re} [\psi^* (-i\nabla - \mathbf{A}) \psi] - \kappa^2 \text{rot rot} \mathbf{A}. \quad (3)$$

In these equations, the length was expressed in units of the coherence length  $\xi$  and the vector potential is scaled to  $\Phi_0/(2\pi\xi)$  (where  $\Phi_0$  is the magnetic flux quantum). Time is in units of the



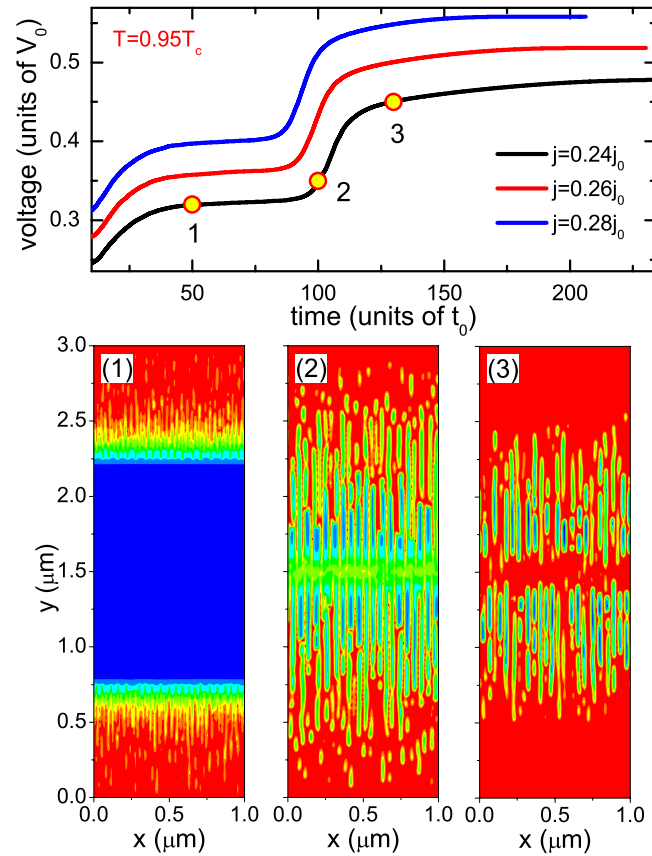


FIG. 4. Theoretical voltage vs. time of the sample at  $T = 0.95 T_c$  for different values of the applied current density  $j$ . It shows clearly three regimes, a flux flow regime which precedes  $t_d$ , followed by the nucleation of a PSC quickly transformed into a HS whose voltage saturates as the whole film becomes normal. Panels 1-3 show the snapshots of the Cooper-pair density  $|\psi|^2$  (blue and red corresponds respectively to 1 and 0 value of the superconducting order parameter) at times indicated in the  $V(t)$  curves.

Ginzburg-Landau relaxation time  $t_0 = 4\pi\lambda^2/c^2\rho_n$  ( $\rho_n$  is the normal-state resistivity,  $c$  is the velocity of light), the voltage is in units of  $V_0 = c\Phi_0\rho_n/8\pi^2\lambda^2\xi$  and the current density is measured in units of  $j_0 = c\Phi_0/8\pi^2\lambda^2\xi$ . The parameters  $u$  and  $\gamma$ , which are the measures of the different relaxation times, are taken as  $u = 5.79$  and  $\gamma = 10$ .<sup>12</sup> Using  $\xi(0) = 2$  nm,  $\lambda(0) = 100$  nm and  $\rho_n = 186 \mu\Omega\cdot\text{cm}$ , which are typical for the experimental sample, we obtain  $t_0 \approx 0.1$  ps and  $V_0 \approx 3$  mV at  $T = 0.83 T_c$ . Since the film measured is relatively thick (150 nm), we can neglect the demagnetization effects due to the magnetic field of the current.<sup>11</sup> These coupled nonlinear differential equations are solved self-consistently following the numerical approach of Ref. 13. Periodic boundary conditions are used along the length and Neumann boundary conditions along the width and for  $\kappa = 10$ .

A superconducting part of the film with width  $w = 3 \mu\text{m}$  and period  $L = 1 \mu\text{m}$ , and current pulse duration  $\Delta t = 5000 t_0$  is applied at  $t = 2 t_0$ . Fig. 4 shows the voltage response of this part of the film to different values of the current density  $j$  and at temperature  $T = 0.95 T_c$ . When the applied current increases but still below the critical current  $I_c$  as defined previously, vortices and antivortices are created at the opposite edges of the sample due to the magnetic field of the current (panel 1 in Fig. 4 in red color). They move towards the middle of the sample where they annihilate (panel 2 of Fig. 4). When the current is increased, the output voltage increases due to the formation of a phase-slip line after a certain delay time  $t_d$  (panel 3 of Fig. 4). The delay time  $t_d$  is reduced with increasing the current amplitude, and it is reproduced by our experiment in Fig. 2 and 3. The output voltage becomes constant in the phase slip regime, and this behaviour was shown in Fig. 2 where saturation of the voltage versus time is reached. The flux flow was not seen in Fig. 2(a)

before the PSC delay time, due the pinning of the vortices at  $T \ll T_c$ . However, it was clearly seen experimentally in the case of high- $T_c$  superconductors.<sup>14,15</sup> Further increase of the applied current led to the transformation of PSC to HS, which in the present geometry (finite length  $L$ ) means a complete transition to the normal state and saturating voltage. Experimentally, one observes a monotonous increase of the voltage  $v$ s  $t$ , which does not saturate for a long filament.

## V. CONCLUSION

We have studied the transport properties of NbTiN superconducting film at 4.2 K, using a current pulse technique. In response to a super-critical current the dissipative modes namely HS and PSC, were reported in two different samples. The heat escape times was subsequently determined from the delay before the appearance of a PSC or a HS. This parameter plays an important role in determining the limiting performance of the superconducting single photon detectors. In addition, a numerical simulation, based on the resolution of the time-dependent Ginzburg-Landau equations, showed that some important experimental facts could be reproduced. Different types of dissipation such as the vortex flow regime without delay, and the delayed PSC nucleation and HS formation were unambiguously depicted.

## ACKNOWLEDGMENTS

K.H gratefully acknowledges the support of the King Fahd University of Petroleum and Minerals, Saudi Arabia, under the IN131034 DSR project.

- <sup>1</sup> G. N. Gol'tsman, O. Okunev, G. Chulkova, A. Lipatov, A. Semenov, K. Smirnov, B. Voronov, A. Dzardanov, C. Williams, and Roman Sobolewski, *App. Phys. Lett.* **79**, 705 (2001).
- <sup>2</sup> M. Ejrnaes *et al.*, *Supercond. Sci. Technol.* **22**, 055006 (2009).
- <sup>3</sup> M. Tinkham, *Intro. to Superconductivity*, 2nd ed. (McGraw-Hill, Singapore, 1996), Chap. 11.
- <sup>4</sup> M. Tinkham, in *Non-Equilibrium Superconductivity, Phonons and Kapitza Boundaries*, edited by K.E. Gray (Plenum, New York, 1981), pp. 231-262.
- <sup>5</sup> K. Harrabi, F.R. Ladan, Vu Dinh Lam, J.-P. Maneval, J.-F. Hamet, J.-P. Villégier, and R.W. Bland, *J. Low Temp. Phys.* **157**, 36 (2009).
- <sup>6</sup> F.-R. Ladan, Kh. Harrabi, M. Rosticher, C. Villard, P. Mathieu, and J.-P. Maneval, *J. Low Temp. Phys.* **153**, 103 (2008).
- <sup>7</sup> K. Harrabi, N. Cheenne, V. D. Lam, F. R. Ladan, and J. P. Maneval, *J. Supercond.* **14**, 325 (2001).
- <sup>8</sup> K. Harrabi, A.F. Salem, K. Ziq, A. Mansour, S. Kunwar, G. Berdiyurov, and J.P. Maneval, *Appl. Phys. A* **117**, 2033 (2014).
- <sup>9</sup> W.J. Skocpol, M.R. Beasley, and M. Tinkham, *J. Low Temp. Phys.* **16**, 145 (1974).
- <sup>10</sup> J.A. Pals and J. Wolter, *Phys. Lett. A* **70**, 150 (1979).
- <sup>11</sup> G. Berdiyurov, K. Harrabi, F. Oktasendra, K. Gasmi, A. I. Mansour, J.P. Maneval, and F. M. Peeters, *Phys. Rev. B* **90**, 134505 (2014).
- <sup>12</sup> L. Kramer and R. J. Watts-Tobin, *Phys. Rev. Lett.* **40**, 1041 (1978); R. J. Watts-Tobin, Y. Krähenbühl, and L. Kramer, *J. Low Temp. Phys.* **42**, 459 (1981).
- <sup>13</sup> D. Yu. Vodolazov and F. M. Peeters, *Phys. Rev. B* **76**, 014521 (2007).
- <sup>14</sup> K. Harrabi, *J. Supercond. Nov. Magn.* **26**, 1865 (2013).
- <sup>15</sup> K. Harrabi, *J. Supercond. Nov. Magn.* DOI <http://dx.doi.org/10.1007/s10948-014-2691-0> (2014).